





 Cite this: *RSC Adv.*, 2021, 11, 31791

 Received 6th July 2021
 Accepted 10th September 2021

DOI: 10.1039/d1ra05199g

rsc.li/rsc-advances

pH sensing and bioimaging using green synthesized carbon dots from black fungus†

 Jing Qin,‡ Xu Gao,  ‡ Qinqin Chen, Huiling Liu, Shuqi Liu, Juan Hou * and Tiedong Sun *

Biomass is regarded as an excellent candidate for the preparation of carbon nanomaterials. A pH sensor was established based on carbon dots synthesized from black fungus, and possesses good fluorescence response and reversibility for pH detection. Meanwhile, the CDs can also be applied to intra-cellular bioimaging, showing potential for bioimaging.

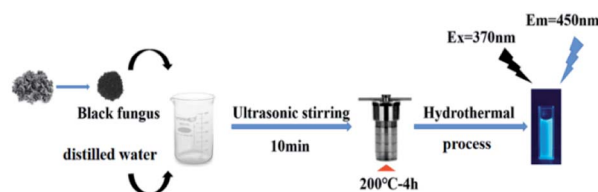
Carbon dots (CDs) are spherical fluorescent nanoparticles with sizes less than 10 nm.¹ Due to their attractive properties of high chemical stability, bright fluorescence, water solubility, facile synthesis and easy modification, CDs have attracted lots of attention in recent years. Many works revealed green synthetic approaches of CDs from renewable or natural materials and have advantages such as non-toxicity, economic production, cleanliness and facile accessibility.^{2,3} For example, banana,^{4,5} eggshell membrane,⁶ roasted chickpeas,⁷ tapioca flour,⁸ spinach,⁹ green tea leaf residue,¹⁰ pea¹¹ and betel leaves¹² have all been utilized as carbon precursors. The main synthesis approaches could be classified into two categories, top-down and bottom-up strategies. The top-down method refers to cutting down large carbon materials into fine nanoparticles by acid etching or laser cauterization.¹³ While, the bottom-up method involves chemically fusing organic molecules *via* carbonization and dehydration under thermal/hydrothermal/solvothermal conditions, which is effective and simple. A hydrothermal method has been proved to be facile and rapid for CD fabrication.¹⁴ CDs can be directly obtained from various green materials under high temperature and pressure conditions. The as-prepared CDs, as promising fluorescent materials, were applied widely in many practical applications including biological labeling, optoelectronic devices, biosensors, gene delivery, drug delivery, antimicrobial coating and so on, showing their potential in replacing heavy metal-doped quantum dots and organic dyes.^{15–20}

The pH value plays an important role in both environmental and biological processes. Slight change of intracellular pH can also lead to organ damage or neurological problems. Recently,

fluorescent CDs-based nanosensors have been established for the pH detection in environmental samples and *vivo/vitro* bio-analysis.²¹ In this communication, blue-emissive CDs with good biocompatibility and high fluorescence were fabricated by facile hydrothermal treatment of black fungus at 200 °C. The obtained CDs were utilized in pH determination and cell imaging for preliminary study.²²

The CDs were synthesized *via* a rapid and low-cost hydrothermal treatment using black fungus as the carbon precursor. The black fungus was grounded and mixed with distilled water. The mixture was then poured into a 50 mL Teflon reaction vessel and autoclaved at 200 °C for 4 h. After cooling to room temperature, the reaction yielded a kind of brown solution with strong blue fluorescence. After purification by filter and dialysis, pure CDs were obtained. The products could also be dried to solid by freeze-drying. Full details for the preparation conditions optimization (reaction time and temperature of the hydrothermal treatment) were listed in the ESI† (Tables S1 and S2). Under the same preparation conditions, the reaction phenomena were consistent with different batches. The overall scheme of the preparation of CDs derived from black fungus is presented in Scheme 1.

The CDs were analyzed with high resolution transmission electron microscopy (HRTEM) images to ascertain their morphology. Fig. 1a shows the as-prepared CDs are nearly spherical in shape and well distributed with average sizes of 2.23 nm. The lattice fringes spacing in HRTEM image is



Scheme 1 Schematic illustration of CDs synthesis.

Department of Chemistry, Chemical Engineering and Resource Utilization, Northeast Forestry University, 26 Hexing Road, Harbin 150040, PR China. E-mail: houjuan0503@126.com; tiedongsun@nefu.edu.cn

† Electronic supplementary information (ESI) available. See DOI: 10.1039/d1ra05199g

‡ These authors contributed equally to this work.



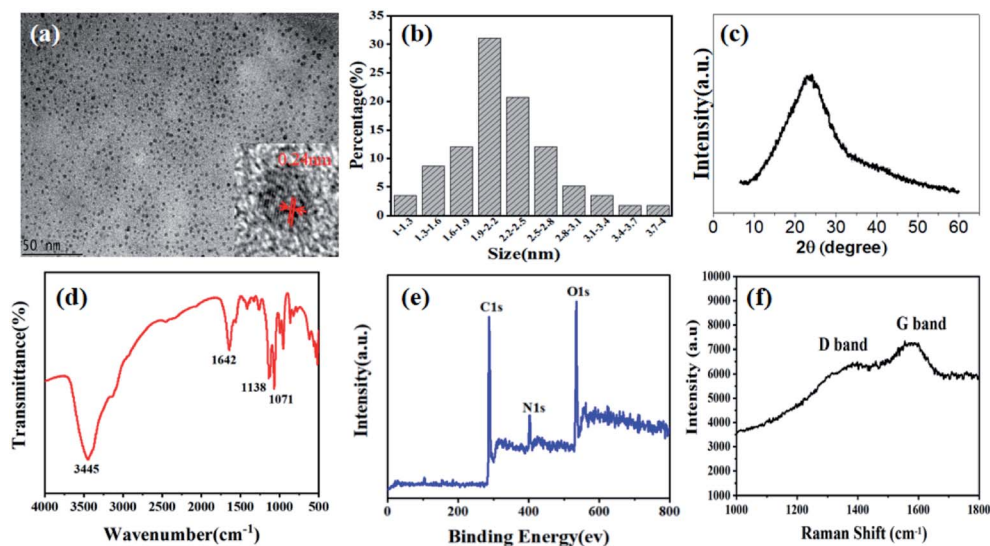


Fig. 1 TEM image (inset: HR-TEM image) (a), particle size distribution (b), XRD pattern (c), FTIR spectrum (d), XPS spectrum (e), and Raman spectrum (f) of the CDs.

observed to be 0.24 nm corresponding to the (1 1 2) facet of graphitic carbon, which indicates good crystallinity of the CDs (Fig. S1† and inset of Fig. 1a). The X-ray diffraction (XRD) pattern in Fig. 1c exhibits a broad peak at about 22.4° , associated with the graphitic structure of the CDs.

Fourier transform infrared spectrum (FTIR) and X-ray photoelectron spectroscopy (XPS) were conducted to confirm the states of the elements and analyze the surface functional groups of the CDs. As shown in Fig. 1d, the characteristic peaks

at 3445, 1642, 1138, 1071 cm^{-1} corresponded to the stretching vibrations of O–H/N–H, asymmetric stretching vibrations of C=N/C=O, aromatic stretching vibrations of C–N and tensile vibrations of C–O. The full range XPS spectrum confirms the main peaks of CDs are C, N, O and S at 284.8, 401.0, 531.5 and 170.4 eV with atomic contents of 64.14%, 10.01%, 24.24%, and 1.61%, respectively, indicating the incorporation of N and S into the carbon matrix. The abundance of proteins in black fungus provides the doping of heteroatoms. The fitted peaks of C_{1s} , N_{1s}

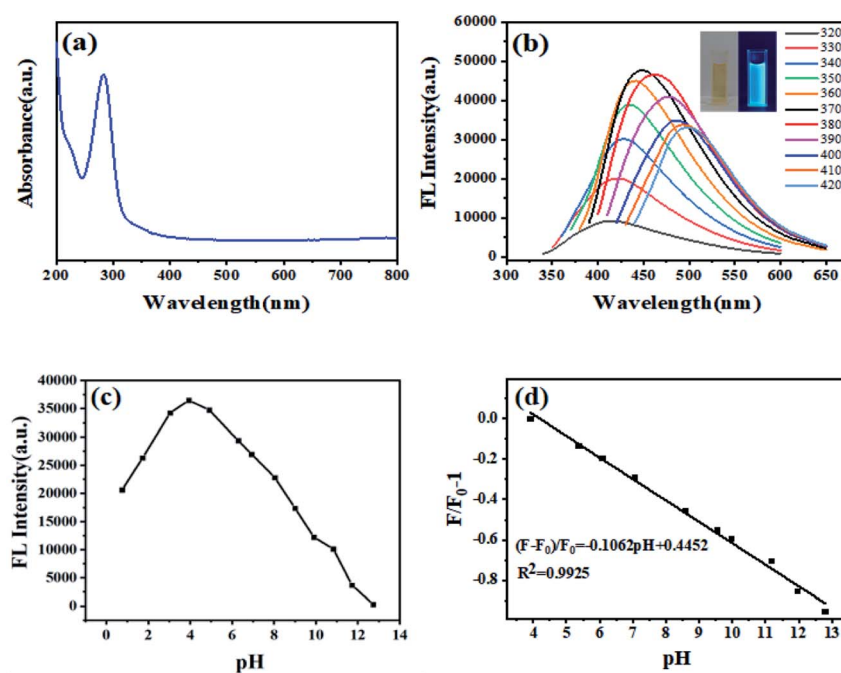


Fig. 2 Absorption spectrum (a), fluorescence emission spectra of CDs: excitation wavelength starts from 320 to 420 nm; inset: photos of the CDs dispersed in water under daylight (left) and UV irradiation (right) (b), the relationship between the FL intensity and pH variation in the range of 1–13 (excited at 370 nm) (c), the fitted linear curve with pH variation around physiological condition (4.0–13.0) (d).

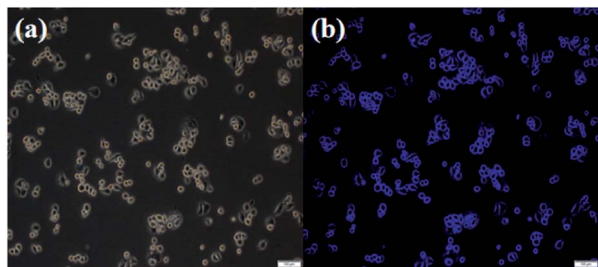


Fig. 3 Bright-field image (a) and the fluorescence image *in vitro* of HeLa cells with CDs (the excitation wavelength was 370 nm) (b).

and O_{1s} were shown in high-resolution XPS to analyze the chemical bonds (Fig. S2†). The C_{1s} spectrum could be deconvoluted into four peaks at 284.0 eV, 284.7 eV, 285.8 eV, 287.5 eV, corresponding to the four kinds of C-bonds, including C=C, C-C, C-N/C-O, C=N/C=O. The O_{1s} spectrum was deconvoluted into two components of C=O (531.5 eV) and C-OH (532.8 eV). The deconvolution of N_{1s} spectrum demonstrated the presence of three types of N-bands: pyridinic N at 398.7 eV, amino N at 399.5 eV and pyrrolic N at 401.1 eV, respectively. The XPS data and FTIR spectrum are in good agreement, which determined that many hydrophilic groups on the surface endow CDs with good water solubility. Raman spectrum is shown in Fig. 1f. The feature centered at 1378 cm^{-1} (D band) implying the sp^3 C-C bands or defects in graphene framework, while the feature centered at 1570 cm^{-1} (G band) indicates the character of sp^2 nature for C=C bands.

The optical properties of the CDs from black fungus were characterized by UV-vis and fluorescence spectroscopy. The absorption spectrum of the CDs in aqueous solution was shown in Fig. 2a. The peaks at 230 nm and 282 nm are ascribed to the $\pi-\pi^*$ of C=C bonds and $n-\pi^*$ of C=C/C=O bonds transitions,²³ respectively. The fluorescence spectra of as-prepared CDs excited by different wavelengths are shown in Fig. 2b. The as-prepared CDs demonstrated excitation-dependent FL behavior, which approximates to reported literatures of CDs.²⁴ Increasing the excitation wavelength from 320 nm to 420 nm, the emission peak red-shifts gradually. At 370 nm excitation, the CDs show highest intensity at emission peak of 450 nm (Fig. S3†). The CDs solution emitted bright blue fluorescence under irradiation of 365 nm UV lamp (Fig. 2b, inset), which can be used as invisible ink for information encryption or painting patterns (Fig. S4†). The fluorescence quantum yield of as-prepared CDs was estimated to be 11.3% by the direct measurement, which is comparable with other reported CDs derived from biomass (Table S3†).

The stability of CDs under different conditions was investigated as shown in Fig. S5.† Although the FL intensity of CDs was slightly affected by NaCl concentrations, there was still above 90% of intensity in a NaCl solution with a high concentration of 2.0 M (Fig. S5a†). The effect of exposure time on FL intensity was shown in Fig. S5b.† It can be found that the FL intensity remained negligible change after continuous 365 nm UV exposure of 60 min, indicating good photobleaching resistance.

Moreover, after long time storage for 20 days, the CDs solutions showed little effect, suggesting good time stability (Fig. S5c†).

The CDs exhibited an obvious pH-sensitive FL property due to the protonation-deprotonation of the surface functional groups. Fig. 2c depicts the effects of solution pH value on the FL intensity at the emission wavelength of 450 nm when excited at 370 nm. The FL intensity of as-prepared CDs has an incredibly fast response to the change of solution pH value. Increasing the pH value from 1–13, the intensity of CDs showed an increasing trend from pH 1 to 4 and then decreases gradually. There is an excellent linear relationship between the FL intensity and the pH value with a pH range from 4–13. The linear regression equation is $(F - F_0)/F_0 = -0.1062\text{ pH} + 0.4452$ and the linear dependence coefficient (R^2) is 0.9925. After 5 times of changing pH value from 5 to 11 and then back to 5, the FL intensity does not show apparent change from the original value under the same solution pH conditions, demonstrating good pH reversible performance and response ability of the CDs (Fig. S6†). A series of control experiments were carried out to evaluate the sensitivity and selectivity of the CDs when used as the pH detection probe. Unlike significant fluorescence changes with adjusting the pH value of CDs solution, common cations, anions and compounds showed negligible effect on the fluorescence intensity, indicating excellent selectivity to pH values (Fig. S7†). Therefore, the CDs can be served as potential pH sensor in both environmental samples or biological systems. As illustrated in Table S4,† different samples were taken as analytical models. The results calculated by the proposed CDs-based probe and measured by pH-meter are basically the same.

In view of good fluorescence properties of the CDs, the fluorescence imaging *in vitro* was conducted. HeLa cells were used as the model system to investigate the cytotoxicity of CDs. The toxicity of the obtained CDs towards HeLa cells could be negligible even after 48 h. The cell viability was higher than 80% at a high concentration of $800\text{ }\mu\text{g mL}^{-1}$. The HeLa cells were cocultured with the as-prepared CDs ($100\text{ }\mu\text{g mL}^{-1}$) at $37\text{ }^\circ\text{C}$ for 4 h and then subjected to the confocal fluorescence imaging (Fig. 3). Bright blue fluorescence signal of the cells could be observed, which demonstrates that the CDs have potential applications in biological imaging. To further investigate the biocompatibility of the as-prepared CDs, we conducted the hydroponics experiments of soybeans with CDs solutions. We grew soybeans sprouts using CDs aqueous solution. After incubation for 3–4 days at room temperature, the soybeans have sprouted normally, and their sprouts displayed blue fluorescence emissions under UV light (365 nm), demonstrating that the CDs were non-toxic and easily taken into the soybeans (Fig. S8†). Therefore, the obtained CDs have good biocompatibility.

Conclusions

In summary, we fabricated bright blue-emissive CDs by a simple hydrothermal treatment from natural materials (black fungus). The as-prepared CDs showed uniform morphology, good fluorescence properties, FL stability, low toxicity and excellent biocompatibility. Preliminary investigation implies that the

CDs exhibit good pH reversible performance and FL response ability. A pH-sensor based on the CDs has been established and applied to real sample analysis with satisfactory results. Moreover, the CDs also can be used in intra-cellular bioimaging, implying potential in biomedical and bioimaging fields.

Conflicts of interest

There are no conflicts to declare.

Acknowledgements

We gratefully acknowledge the support from National Natural Science Foundation of China (NSFC, No. 21804017), China Postdoctoral Science Foundation (No. 2019M651242), and Heilongjiang Postdoctoral Science Fund (LBH-Z18009).

Notes and references

- 1 B. Xue, Y. Yang, Y. Sun, J. Fan, X. Li and Z. Zhang, *Int. J. Biol. Macromol.*, 2019, **122**, 954–961.
- 2 R. Kumar, V. B. Kumar and A. Gedanken, *Ultrason. Sonochem.*, 2020, **64**, 105009.
- 3 Y. Choi, X. T. Zheng and Y. N. Tan, *Mol. Syst. Des. Eng.*, 2020, **5**, 67–90.
- 4 N. Chaudhary, P. K. Gupta, S. Eremin and P. R. Solanki, *J. Environ. Chem. Eng.*, 2020, **8**, 103720.
- 5 R. Atchudan, T. N. J. I. Edison, S. Perumal, N. Muthuchamy and Y. R. Lee, *Fuel*, 2020, **275**, 117821.
- 6 Z. Ye, Y. Zhang, G. Li and B. Li, *Anal. Lett.*, 2020, **53**, 2841–2853.
- 7 A. Başoğlu, Ü. Ocak and A. Gümrükçüoğlu, *J. Fluoresc.*, 2020, **30**, 515–526.
- 8 M. Y. Pudza, Z. Z. Abidin, S. A. Rashid, F. M. Yasin, A. S. M. Noor and M. A. Issa, *Nanomaterials*, 2020, **10**, 315.
- 9 X. Xu, L. Cai, G. Hu, L. Mo, Y. Zheng, C. Hu, B. Lei, X. Zhang, Y. Liu and J. Zhuang, *J. Lumin.*, 2020, **227**, 117534.
- 10 Z. Hu, X.-Y. Jiao and L. Xu, *Microchem. J.*, 2020, **154**, 104588.
- 11 Q. Su, L. Gan, J. Liu and X. Yang, *Anal. Biochem.*, 2020, **589**, 113476.
- 12 R. Atchudan, T. N. J. I. Edison, S. Perumal, R. Vinodh and Y. R. Lee, *J. Mol. Liq.*, 2019, **296**, 111817.
- 13 Z. Li, L. Wang, Y. Li, Y. Feng and W. Feng, *Mater. Chem. Front.*, 2019, **3**, 2571–2601.
- 14 R. Sendão, M. d. V. M. d. Yuso, M. Algarra, J. C. G. Esteves da Silva and L. Pinto da Silva, *J. Cleaner Prod.*, 2020, **254**, 120080.
- 15 Q. Ye, F. Yan, Y. Luo, Y. Wang, X. Zhou and L. Chen, *Spectrochim. Acta, Part A*, 2017, **173**, 854–862.
- 16 A. Nair, J. T. Haponiuk, S. Thomas and S. Gopi, *Biomed. Pharmacother.*, 2020, **132**, 110834.
- 17 M. Pirsaeheb, S. Mohammadi and A. Salimi, *TrAC, Trends Anal. Chem.*, 2019, **115**, 83–99.
- 18 Q. Yang, J. Duan, W. Yang, X. Li, J. Mo, P. Yang and Q. Tang, *Appl. Surf. Sci.*, 2018, **434**, 1079–1085.
- 19 C. Zhang, Y. Xiao, Y. Ma, B. Li, Z. Liu, C. Lu, X. Liu, Y. Wei, Z. Zhu and Y. Zhang, *J. Photochem. Photobiol., B*, 2017, **174**, 315–322.
- 20 X.-a. Zhang, W. Zhang, Q. Wang, J. Wang, G. Ren and X.-d. Wang, *Microchim. Acta*, 2019, **186**, 584.
- 21 X. Wang, Y. Wang, W. Pan, J. Wang and X. Sun, *ACS Sustainable Chem. Eng.*, 2021, **9**, 3718–3726.
- 22 S. Chang, B. B. Chen, J. Lv, E. K. Fodjo, R. C. Qian and D. W. Li, *Microchim. Acta*, 2020, **187**, 435.
- 23 Q. Li, Z. Bai, X. Xi, Z. Guo, C. Liu, X. Liu, X. Zhao, Z. Li, Y. Cheng and Y. Wei, *Spectrochim. Acta, Part A*, 2021, **248**, 119208.
- 24 P. Chen, J. Zhang, X. He, Y.-H. Liu and X.-Q. Yu, *Biomater. Sci.*, 2020, **8**, 3730–3740.